



The last glaciation of Bear Peninsula, central Amundsen Sea Embayment of Antarctica: Constraints on timing and duration revealed by *in situ* cosmogenic ^{14}C and ^{10}Be dating



Joanne S. Johnson^{a,*}, James A. Smith^a, Joerg M. Schaefer^b, Nicolás E. Young^b, Brent M. Goehring^c, Claus-Dieter Hillenbrand^a, Jennifer L. Lamp^b, Robert C. Finkel^d, Karsten Gohl^e

^a British Antarctic Survey, High Cross, Madingley Road, Cambridge CB3 0ET, UK

^b Lamont-Doherty Earth Observatory, Columbia University, Route 9W, Palisades, New York NY 10964, USA

^c Department of Earth & Environmental Sciences, Tulane University, New Orleans, LA 70118, USA

^d Lawrence Livermore National Laboratory, Center for Accelerator Mass Spectrometry, 7000 East Avenue Avenue, Livermore, CA 94550-9234, USA

^e Alfred Wegener Institute for Polar and Marine Research, Postfach 120161, D-27515 Bremerhaven, Germany

ARTICLE INFO

Article history:

Received 6 April 2017

Received in revised form

18 October 2017

Accepted 1 November 2017

Keywords:

Quaternary

Glaciology

Antarctica

Cosmogenic isotopes

Geomorphology

Glacial

Amundsen Sea Embayment

In-situ ^{14}C

Ice streams

ABSTRACT

Ice streams in the Pine Island-Thwaites region of West Antarctica currently dominate contributions to sea level rise from the Antarctic ice sheet. Predictions of future ice-mass loss from this area rely on physical models that are validated with geological constraints on past extent, thickness and timing of ice cover. However, terrestrial records of ice sheet history from the region remain sparse, resulting in significant model uncertainties. We report glacial-geological evidence for the duration and timing of the last glaciation of Hunt Bluff, in the central Amundsen Sea Embayment. A multi-nuclide approach was used, measuring cosmogenic ^{10}Be and *in situ* ^{14}C in bedrock surfaces and a perched erratic cobble. Bedrock ^{10}Be ages (118–144 ka) reflect multiple periods of exposure and ice-cover, not continuous exposure since the last interglacial as had previously been hypothesized. *In situ* ^{14}C dating suggests that the last glaciation of Hunt Bluff did not start until 21.1 ± 5.8 ka – probably during the Last Glacial Maximum – and finished by 9.6 ± 0.9 ka, at the same time as ice sheet retreat from the continental shelf was complete. Thickening of ice at Hunt Bluff most likely post-dated the maximum extent of grounded ice on the outer continental shelf. Flow re-organisation provides a possible explanation for this, with the date for onset of ice-cover at Hunt Bluff providing a minimum age for the timing of convergence of the Dotson and Getz tributaries to form a single palaeo-ice stream. This is the first time that timing of onset of ice cover has been constrained in the Amundsen Sea Embayment.

© 2017 The Authors. Published by Elsevier Ltd. This is an open access article under the CC BY license (<http://creativecommons.org/licenses/by/4.0/>).

1. Introduction

Ice mass loss from the Pine Island-Thwaites drainage basins of the Amundsen Sea sector presently dominates the Antarctic contribution to global sea level (Shepherd et al., 2012; King et al., 2012), and research has therefore focused on this region (e.g. Joughin and Alley, 2011; Alley et al., 2015). However, despite their comparably high contemporary rates of grounding line retreat, thinning, and flow acceleration (Pritchard et al., 2009; Rignot et al.,

2014; Mouginot et al., 2014), ice streams draining the central Amundsen Sea Embayment (ASE; Fig. 1) have received less attention. This is particularly apparent over the longer timescales required for evaluation of ice sheet response to climate forcings: whilst millennial-scale ice sheet reconstructions for the Pine Island sector of the West Antarctic Ice Sheet (WAIS) have improved significantly in the last decade, (e.g. Kirshner et al., 2012; Hillenbrand et al., 2013; Smith et al., 2014; Johnson et al., 2008, 2014), there is still only a very sparse understanding of glacial history of the Thwaites sector (Larter et al., 2014). In particular, the magnitude and timing of past thinning of the Pope, Smith and Kohler Glaciers – which presently drain the Thwaites Glacier catchment – remain largely unknown even though models predict

* Corresponding author.

E-mail address: jsj@bas.ac.uk (J.S. Johnson).

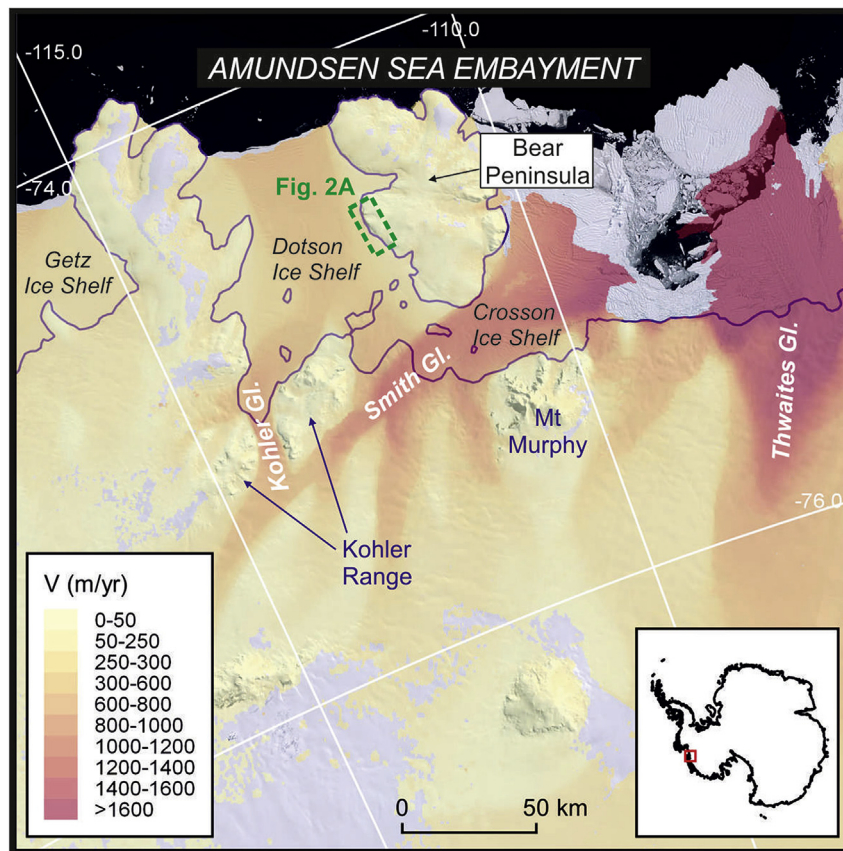


Fig. 1. Location of Bear Peninsula and surrounding ice streams of the central Amundsen Sea Embayment. Ice velocities (V ; Rignot et al., 2011a,b) are overlain on the Landsat Image of Antarctica (LIMA). The 2011 grounding line shown is from Rignot et al. (2011c); using their preferred approach for determining grounding line position, Bear Peninsula is an island, whereas previous studies show it as a peninsula. The inset shows location of the figure in relation to the rest of Antarctica. The dashed green box denotes Hunt Bluff, from where our samples were collected. Fig. 2A shows that area in more detail. (For interpretation of the references to colour in this figure legend, the reader is referred to the web version of this article.)

that this region will dominate the Antarctic contribution to sea level rise by the year 2100 (Ritz et al., 2015). In order to better constrain ice sheet history of the region and improve reconstruction of its past ice dynamics in physical models, here we provide glacial-geological evidence of the timing – both onset and final deglaciation – of the last glacial cover in the central ASE from a site adjacent to the Dotson Ice Shelf (Fig. 1).

2. Late Quaternary ice sheet history

The configuration of WAIS in the central ASE during the last glacial cycle was summarized by Larter et al. (2014). Their review showed that, whilst the deglacial history of the Dotson-Getz palaeo-ice stream, which formerly drained the coast of Marie Byrd Land outboard of Smith Glacier, is relatively well-understood (Smith et al., 2011), there are only very sparse *terrestrial* geological data (Johnson et al., 2008; Lindow et al., 2014) constraining ice sheet thickness in the area since the Last Glacial Maximum (LGM).

Substantial progress in reconstructing late Quaternary ice sheet history of the ASE has been made over the past decade in the marine realm. Subglacial bedforms detected using multibeam bathymetry and deglacial ages from marine sediment cores provide evidence that the WAIS extended to the edge of the continental shelf across most of the ASE at the LGM (Graham et al., 2010; Kirshner et al., 2012; Larter et al., 2009; Smith et al., 2011, 2014). Radiocarbon dating of marine sediment cores in the outer Dotson-Getz Trough revealed that deglaciation of the western ASE was

underway by 22.4 cal kyr BP (Smith et al., 2011). The grounding line then retreated rapidly across the middle and inner shelf from 13.8 cal kyr BP arriving within 12 km of the present front of the Dotson Ice Shelf by 11.4 cal kyr BP (Smith et al., 2011). This behaviour is roughly contemporaneous with retreat close to other ice shelf fronts in the ASE; a compilation of deglacial ages from marine sediment cores showed that WAIS retreat from the whole ASE shelf was largely complete by the start of the Holocene (Hillenbrand et al., 2013).

The only *terrestrial* studies from the central ASE report five cosmogenic ^{10}Be exposure ages on erratic cobbles from two nunataks in the Kohler Range (Fig. 1; Lindow et al., 2014) and paired ^{10}Be - ^{26}Al for a striated bedrock sample from Hunt Bluff on Bear Peninsula (Fig. 1; Johnson et al., 2008). We have recalculated these, and all other previously-published exposure ages discussed in this paper, using the same production rate and scaling factor to allow direct comparison with our new results (see section 5: Methods). The erratic ages suggest that nunataks in the Kohler Range were deglaciated between 13.4 ± 0.6 and 8.7 ± 0.4 ka (Lindow et al., 2014). This is consistent with the broader deglacial chronology provided by the marine data from the Dotson-Getz palaeo-ice stream, suggesting that those nunataks became ice-free around the same time that WAIS had finished its last retreat across the continental shelf (i.e. during the early Holocene; cf. Hillenbrand et al., 2013). In contrast, the bedrock sample from Bear Peninsula yielded a much older ^{10}Be age, 119.0 ± 3.8 ka (sample HB1; Johnson et al., 2008), potentially suggesting that the site had been

continuously ice-free since that time. However, this age may not represent the timing of the last deglaciation of Hunt Bluff because ^{10}Be and ^{26}Al measurements in Antarctic bedrock are often influenced by inheritance from prior exposure, even when the bedrock is striated (e.g. Hein et al., 2011; Balco, 2011). Thus the question of whether or not WAIS covered all nunataks in the central ASE during the LGM remains unresolved.

3. Rationale

This study focuses on determining the deglacial history of presently exposed bedrock at Hunt Bluff, which is situated on the west side of Bear Peninsula, 140 km north-west of Thwaites Glacier and adjacent to the Dotson Ice Shelf (Fig. 1). There is evidence for rapid recent change in the ice dynamics of this region. For example, disappearing ice rumpled suggest that the Dotson Ice Shelf is now thinning and unpinning from its anchoring points (Rignot et al., 2014), and rapid increases in flow velocity and grounding line retreat of the Smith/Kohler Glacier have been observed over the past two decades (e.g. Rignot et al., 2014). The exposure history of nunataks near both glaciers and the Dotson Ice Shelf will help to place these recent changes into the context of the millennial-centennial scale history of the WAIS, thereby improving the reliability of physical models of past ice sheet change (e.g. Briggs and Tarasov, 2013; Pollard et al., 2016).

Following a brief reconnaissance visit by to Bear Peninsula in 2006, it was hypothesized that Hunt Bluff has been continuously ice-free from at least the last interglacial period of Marine Isotope Stage (MIS) 5 (130–114 ka; Lisiecki and Raymo, 2005), through the LGM to the present-day (Johnson et al., 2008); this was based on results from a single bedrock sample. Here we seek to verify this result, and furthermore, to determine whether Hunt Bluff was ice-free during the LGM.

4. Study area

Bear Peninsula is situated in the central part of the Amundsen Sea Embayment, 140 km west of Thwaites Glacier, and adjacent to the Dotson and Crosson Ice Shelves (Fig. 1). A recent compilation of bedrock topography shows that it is in fact an island, not a peninsula, and is separated from the Antarctic continent by a deep NE-SW trending trough currently occupied by Smith Glacier (Fretwell et al., 2013). With the exception of a few small ice-free areas along its western margin, it is presently almost completely covered by ice. Its topography is dissected by several small glaciers radiating outward to the east and west, draining into the adjacent ice shelves. The Dotson Ice Shelf is fed by the Smith/Kohler Glacier which bifurcates to flow northeastward around the Kohler Range (Fretwell et al., 2013; Rignot et al., 2014). Crosson Ice Shelf, on the eastern side of Bear Peninsula, currently buttresses flow from the major ice stream, Smith Glacier (Fig. 1). Multibeam bathymetry studies have revealed a deep tributary trough extending seawards from the modern front of Dotson Ice Shelf. This merges on the mid-shelf with two troughs that extend from the modern fronts of the Getz Ice Shelf. Together, these troughs mark the former location of the Dotson-Getz palaeo-ice stream (Larter et al., 2009; Graham et al., 2009).

Hunt Bluff lies on the western side of the peninsula, at 470 m above sea level (asl), and approximately 420 m above the surface of the Dotson Ice Shelf (the present surface elevation of the central part of Dotson Ice Shelf is 57 m asl). It consists of a series of small exposed bedrock knolls, which lie along the edge of a NW-SE trending cliff that rises immediately above the ice shelf (Fig. 2A). The bluff is bounded by small outlet glaciers: Zuniga Glacier and True Glacier at the northern and southern ends, respectively.

Bedrock along the bluff is of granodiorite lithology, and was emplaced approximately 300 Ma (Pankhurst et al., 1998). Some upstanding bedrock surfaces are weakly striated (in a N-S orientation), but in general glacial striations are uncommon. Perched erratic cobbles are present, but scarce, and are either granodiorite (the same lithology as the underlying bedrock) or metasedimentary lithologies. The metasedimentary erratics are quartz-bearing but very fine-grained. No till was observed at any of the sites we visited. Patches of blue ice provide evidence for strong winds that prevent significant build-up of snow and ice.

5. Methods

Geological sampling for this study was undertaken using helicopters flown from the German research vessel RV *Polarstern* in 2010 (this was a second visit to Hunt Bluff, following a reconnaissance visit in 2006, described in Johnson et al., 2008). Samples were collected from 4 bedrock surfaces (samples BR-01, BR-03, BR-04, BR-05) and an erratic cobble perched on bedrock (BR-02) (Fig. 2). These were located within a 15 m² area, at the same location and elevation as a striated bedrock sample dated by Johnson et al. (2008), and of similar granodiorite lithology. The erratic cobble selected for sampling was perched on a near-horizontal bedrock surface, which minimizes the chance that it had turned over or rolled since first becoming exposed.

Cosmogenic ^{10}Be exposure dating was undertaken on all the bedrock and erratic samples, and *in situ* cosmogenic ^{14}C was additionally measured on one bedrock sample (BR-01, which yielded the oldest ^{10}Be age; Table 1) and the erratic cobble (BR-02). Measuring two different nuclides and applying a multi-nuclide approach to bedrock exposure dating can permit determination of complex exposure histories (e.g. Bierman et al., 1999; Fabel et al., 2002; Lilly et al., 2010). However, Johnson et al. (2008) nevertheless found ^{26}Al analysis inconclusive with respect to determining if bedrock from Hunt Bluff experienced a complex exposure history. *In situ* ^{14}C bedrock dating (cf. Miller et al., 2006; Goehring et al., 2011; Briner et al., 2014) was therefore applied to determine if Hunt Bluff experienced multiple phases of glaciation. *In situ* ^{14}C has a much shorter half-life (5730 yr) than ^{10}Be (1.39 Myr; Nishiizumi et al., 2007; Chmeleff et al., 2010; Korschinek et al., 2010) and ^{26}Al (0.7 Myr; Nishiizumi, 2004). Thus any *in situ* ^{14}C acquired during exposure decays to background levels if a surface is subsequently covered by ice for periods longer than 5–6 half-lives (i.e. >~30 kys). At Hunt Bluff, this method allowed determination of whether or not the bedrock surface was ice-covered during the LGM. Furthermore, if a deglaciation age for the site is known (e.g. it has been determined from an erratic perched on the bedrock), the duration of ice cover – and hence an age for onset of that cover – can be calculated. The method and calculations for this approach at Hunt Bluff are described in section 5.3 below.

5.1. Analytical procedures

Samples were prepared for ^{10}Be measurement at Lamont-Doherty Earth Observatory cosmogenic nuclide laboratory (<http://www.ldeo.columbia.edu/res/pi/tcn>) using procedures developed for high-sensitivity ^{10}Be exposure dating (Schaefer et al., 2009). Sample details and ^{10}Be age data are shown in Table 1. Published ^{10}Be (Table 1) and ^{26}Al (Table 2) exposure ages for Hunt Bluff bedrock (Johnson et al., 2008; recalculated for direct comparison) are also included. Analysis of $^{10}\text{Be}/^9\text{Be}$ ratios was undertaken by the Center for Accelerator Mass Spectrometry, Lawrence Livermore National Laboratory, USA. Sample $^{10}\text{Be}/^9\text{Be}$ ratios were measured relative to the 07KNSTD3110 standard, which has a $^{10}\text{Be}/^9\text{Be}$ ratio of 2.85×10^{-12} . ^{10}Be backgrounds, controlled by procedural blanks

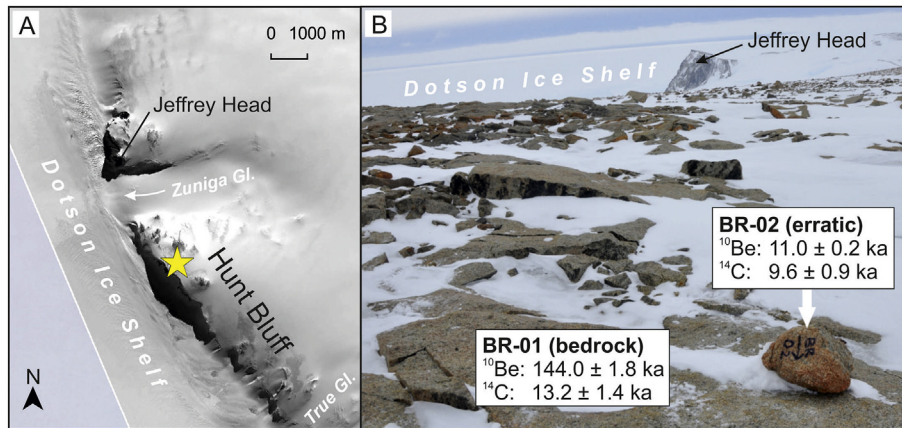


Fig. 2. Sample site at Hunt Bluff on Bear Peninsula. A. Location of sample sites (yellow star) in relation to local glaciers and Dotson Ice Shelf. The area covered by this figure is indicated by the dashed green box in Fig. 1. The underlying satellite image is a quickbird image from Digital Globe, available from Digital Globe (<https://browse.digitalglobe.com>). B. Erratic cobble (BR-02; indicated by white arrow) perched on bedrock surface (BR-01) at Hunt Bluff. Exposure ages are from this study. Bedrock samples BR-03, BR-04, BR-05 (this study) and HB1 (Johnson et al., 2008) were collected from nearby (Table 1). (For interpretation of the references to colour in this figure legend, the reader is referred to the web version of this article.)

(^9Be carrier splits that were treated identically to the samples), were below 10,000 ^{10}Be atoms in total, and hence corrections were less than 1%. Corrections for boron interferences were similarly below 1%. *In situ* ^{14}C was extracted from an approximately 5 g aliquot of the pure quartz used for ^{10}Be analysis of bedrock sample BR-01 and erratic cobble BR-02 at Lamont-Doherty Earth Observatory cosmogenic nuclide laboratory, using the methods described by Goehring et al. (2014). AMS analysis was similarly undertaken by Center for Accelerator Mass Spectrometry, Livermore, USA. Analytical details and ^{14}C age data are shown in Table 3.

5.2. Exposure age calculations

^{10}Be and ^{14}C exposure ages were calculated using the online exposure age calculator formerly known as the CRONUS-Earth online exposure age calculator (Balco et al., 2008). Topographic shielding was determined using the associated online geometric shielding calculator, v. 1.1 (Balco et al., 2008). We employed the scaling model of Lifton et al. (2014; LSDn) because it is physically-based, scaling neutrons, protons and muons independently. For sites in Antarctica, using the LSDn scaling yields smaller systematic biases, particularly at higher elevations, compared with the scaling scheme of Lal (1991)/Stone (2000). Nonetheless, we used the air pressure relationship for Antarctica as discussed in Stone (2000). Production rates for ^{14}C are based on a compilation of surfaces in Antarctica that are saturated with respect to ^{14}C , notably the CRONUS-A intercomparison material (Jull et al., 2015); this provides a long-term Antarctic production rate for ^{14}C . Unfortunately, CRONUS-A is not saturated with respect to ^{10}Be , so cannot be used to derive an Antarctic ^{10}Be production rate. The ^{10}Be production rate from a calibration site in New Zealand (P_{NZ} ; Putnam et al., 2010) was therefore used for the age determinations, since it has a similar time-period of integration and was derived from a site situated relatively proximal to Antarctica. For both nuclides, production rates were recalibrated using the same scaling as for the exposure age determinations. The choice of ^{10}Be production rate does not affect the interpretations in this study, which rely primarily on the new *in situ* ^{14}C data. All ^{10}Be and ^{14}C ages are reported using the LSDn scaling scheme (Lifton et al., 2014), and were calculated assuming zero erosion and a quartz density of 2.7 g cm^{-3} .

Since Hunt Bluff is an exposed bedrock knoll swept by strong

katabatic winds, persistent snow accumulation of more than a few centimetres during the austral summer is unlikely. Therefore a correction for snow cover was not applied to the exposure ages. However, assuming 140 cm snow cover (Arthern et al., 2006) for 6 months of every year, with a snow density of 0.25 g cm^{-3} , cosmic ray attenuation length of 165 g cm^{-3} , and average sample heights above the land surface of 0 and 20 cm (for bedrock samples and the erratic, respectively), the reported ^{10}Be exposure ages would change by only 9.6% (for bedrock) and 8.3% (for the erratic).

5.3. Calculating the age of onset for glaciation

The measured concentration of *in situ* ^{14}C , or indeed any nuclide, is a cumulative signal of exposure and burial. To estimate the duration of the last ice cover at Hunt Bluff, we set up a simple model assuming that the sampled bedrock (BR-01) was saturated with respect to ^{14}C when covered during the LGM ice advance. This requires that the bedrock was continuously exposed for ~ 30 ka prior to initiation of ice cover, an assumption that we consider reasonable given that there is evidence from Adélie penguin colonies in the Ross Sea for open marine conditions in West Antarctica between 43.0 and 27.2 ^{14}C kyr BP (Emslie et al., 2007). Furthermore, ice sheet/ice shelf modelling implies that the West Antarctic Ice Sheet has a tendency to experience relatively rapid transitions into and out of collapsed states, within only a few thousand years (Pollard and DeConto, 2009). If a scenario existed where the bedrock was not saturated with respect to ^{14}C , the duration of ice cover calculated here would be overestimated due to the starting concentration of ^{14}C being lower (to account for the measured concentration at present, i.e. the amount accumulated after deglaciation, ice cover would have to be shorter). The model can be summarized as follows: During ice cover – assuming a sufficient thickness to effectively cease ^{14}C production in the underlying bedrock – the ^{14}C that accumulated during previous periods of exposure decays (we assume cold based non-erosive ice cover), and finally during ice retreat the bedrock is exposed and begins to accumulate ^{14}C again. The measured concentration of ^{14}C at the present-day is thus represented by

$$N_{\text{meas}} = N_{\text{post}} + N_{\text{pre}} \exp(-t_g \lambda_{14}), \quad (1)$$

where N_{meas} is the measured bedrock ^{14}C concentration, N_{post} is the

Table 1
¹⁰Be analytical data and exposure ages from Hunt Bluff.

Sample ID	BAS ID	AMS ID	Type	Latitude (S)	Longitude (W)	Altitude (m a.s.l.)	Thickness (cm)	Shielding factor	Quartz weight (g)	⁹ Be carrier (mg)	¹⁰ Be conc. (at.g ⁻¹)	1σ error (at.g ⁻¹)	¹⁰ Be age (yr)	1σ error ^{int} (yr)	¹⁰ Be/ ⁹ Be standard
§, § indicate blank used															
BR-01 [§]	R9.7.1	BE37476	bedrock	-74.5791	-111.8871	478	10	0.999	15.0415	0.18729	1.140E+06	1.368E+04	144.032	1792	07KNSTD ^a
BR-02 [§]	R9.7.2	BE37477	erratic	-74.5791	-111.8869	477	4.1	0.977	15.0488	0.18708	9.343E+04	1.682E+03	11,048	199	07KNSTD
BR-03 [§]	R9.7.3	BE37478	bedrock	-74.5792	-111.8868	477	6.4	0.945	15.1490	0.18698	9.970E+05	1.196E+04	128,802	1596	07KNSTD
BR-04 ^{§,c}	R9.7.4	BE34672	bedrock	-74.5790	-111.8869	477	4.2	0.999	20.0483	0.18903	1.077E+06	1.991E+04	129,447	2472	07KNSTD
BR-05 [§]	R9.7.5	BE37479	bedrock	-74.5791	-111.8871	477	3.1	1.000	15.1573	0.18739	9.982E+05	1.198E+04	118,441	1464	07KNSTD
HB1 ^b	R5.405.2	b1607	bedrock	-74.5791	-111.8868	470	5	0.999			9.799E+05	3.003E+04	118,995	3757	NIST_27900
Process blanks															
Sample ID	AMS ID		Quartz weight (g)	Carrier added (mg)	¹⁰ Be/ ⁹ Be (measured ratio)	¹⁰ Be (atoms)	1σ	¹⁰ Be/ ⁹ Be standard							
§, § indicate blank used															
BLK1-2014Aug21 [§]	BE37474		0	0.18708	5.8995E-16	2.3541E-16	7400	2900							
Blank_2_2013Jan18 [§]	BE34669		0	0.18821	5.3295E-17	4.0470E-17	700	500							
Blank_3_2012Oct09 [§]	BE34677		0	0.18801	3.0894E-16	9.9465E-17	3900	1300							

^a 07KNSTD3110 standard with reported ratio of 2.85×10^{-12} .

^b Johnson et al. (2008).

^c Average of blanks § and §.

concentration of ¹⁴C accumulated since ice retreat, N_{pre} is the saturation concentration of ¹⁴C at the sample site, t_g is the time of onset of ice cover, and λ_{14} is the ¹⁴C decay constant. In the case of Hunt Bluff, we measured N_{post} directly, using the erratic cobble (BR-02); it could also be determined via independent means (e.g. ¹⁰Be exposure dating, radiocarbon dating, etc.).

For this study, we adopted a Monte Carlo approach to determine the timing of onset of ice cover, t_g , and its uncertainty. For all parameters, we assumed Gaussian distributions and determined t_g for each model realization using a minimization approach. The most likely value for t_g is the mean of all realizations ($n = 5000$), and similarly, the uncertainty is the standard deviation of all realizations. In some cases, negative burial ages result; these were removed prior to determining summary statistics.

6. Results

The four new bedrock samples yielded ¹⁰Be ages in the range 118.4 ± 1.5 to 144.0 ± 1.8 ka. When recalculated, the single ¹⁰Be age (119.0 ± 3.8 ka; Table 1) reported by Johnson et al. (2008) falls within this range. We therefore conclude that it is representative of the bedrock ¹⁰Be concentration at Hunt Bluff, and include the age in our dataset and subsequent discussions. In contrast, the erratic cobble, BR-02, yielded a ¹⁰Be exposure age of 11.0 ± 0.2 ka. This is significantly younger than the >100 ka ages for the bedrock on which it was perched – which span the latter stages of the penultimate glacial period, MIS 6 (191–130 ka; Lisiecki and Raymo, 2005) and the early part of the last peak interglacial period, MIS 5e (130–114 ka). Sample BR-01 yielded an *in situ* ¹⁴C age of 13.2 ± 1.4 ka, which is broadly consistent with both the ¹⁰Be and ¹⁴C ages obtained for the erratic cobble (11.0 ± 0.2 ka and 9.6 ± 0.9 ka, respectively), but much younger than its ¹⁰Be age (144.0 ± 1.8 ka). We consider the younger of the two erratic ages (9.6 ± 0.9 ka, from ¹⁴C dating) to be the most representative of the timing of deglaciation of Hunt Bluff, because ¹⁴C is much less likely than ¹⁰Be to reflect nuclide inheritance from a prior period of exposure and is also less sensitive to erosion. The erratic ages correspond closely with the early Holocene ¹⁰Be exposure ages for deglaciation of peaks in the nearby Kohler Range (13.4–8.7 ka; recalculated from Lindow et al., 2014), as well as with the minimum radiocarbon age for retreat of WAIS near to both the present Dotson Ice Shelf front (11.4 cal kyr BP; Smith et al., 2011) and other fringing ice shelves in the ASE (e.g. 10.2 cal kyr BP for Getz A, 12.5 cal kyr BP for Getz B, Smith et al., 2011; 11.7 cal kyr BP for Pine Island, Hillenbrand et al., 2013).

Results of our Monte Carlo simulation of the timing of LGM ice cover are shown in Fig. 3. The ¹⁴C measurements in the erratic cobble and bedrock suggest that Hunt Bluff last became glaciated at 21.1 ± 5.8 ka (the mean and standard deviation of all realizations; Fig. 3A), which coincides with the LGM (Fig. 3B). The cumulative distribution for the Monte Carlo simulation (Fig. 3A) shows that 71% of the realizations resulted in timing estimates for the onset of glaciation after 22.4 ka, which is the date by which grounded ice retreat from the outer continental shelf of the western ASE was underway (Smith et al., 2011). The implications of this result are discussed in section 8.

7. Discussion

Together, the five bedrock ¹⁰Be ages provide a surprisingly internally-consistent dataset given that the degree of inheritance affecting Antarctic bedrock samples is often highly variable (Balco, 2011, and e.g. Hein et al., 2011). Nevertheless, they do not preclude the possibility that the bedrock surfaces experienced a complex exposure history. Pairing ¹⁰Be with ²⁶Al in bedrock from Hunt Bluff

Table 2
Data used to recalculate ^{26}Al exposure age from Hunt Bluff.

Sample ID	BAS ID	AMS ID	Type	Latitude (S)	Longitude (W)	Altitude (m a.s.l.)	Thickness (cm)	Shielding factor	^{26}Al conc. (at.g $^{-1}$)	1σ error (at.g $^{-1}$)	^{26}Al age (yr)	1σ error $^{\text{int}}$ (yr)	$^{26}\text{Al}/^{10}\text{Be}$	^{26}Al standard
HB1 ^a	R5.405.2	a531	bedrock	-74.5791	-111.8868	470	5	0.999	5.984E+06	1.424E+05	110,506	2772	6.11	KNSTD

^a Johnson et al. (2008).

Table 3
In situ ^{14}C analytical data and exposure ages from Hunt Bluff.

Sample ID	BAS ID	AMS ID	Type	Latitude (S)	Longitude (W)	Altitude (m a.s.l.)	Thickness (cm)	Shielding factor	Fraction modern measured	Total ^{14}C atoms blank corrected	1σ error	^{14}C conc. (at.g $^{-1}$)	1σ error (at.g $^{-1}$)	^{14}C age (yr)	1σ error $^{\text{int}}$ (yr)
BR-01	R9.7.1	172628	bedrock	-74.5791	-111.8871	478	10	0.999	0.0278	1,003,062	41,537	199,797	8274	13,199	1353
BR-02	R9.7.2	177406	erratic	-74.5791	-111.8869	477	4.1	0.977	0.0266	895,389	41,804	177,421	8283	9593	850

to determine whether or not the site experienced multiple phases of ice sheet cover has also proved inconclusive (when plotted on a two-isotope diagram – ^{10}Be versus $^{26}\text{Al}/^{10}\text{Be}$ – the sample analysed by Johnson et al., 2008, overlaps the erosion island, meaning that neither continuous exposure nor intermittent shielding by ice can be ruled out). Many Antarctic studies have alternatively favoured analysing erratic cobbles for studies of deglacial history (e.g. Stone et al., 2003; Mackintosh et al., 2007; Bentley et al., 2010; Johnson et al., 2014; Spector et al., 2017). Glacial erratics are very scarce on Bear Peninsula, so a large-scale study was not possible. However, the ^{10}Be and ^{14}C exposure ages from erratic cobble BR-02 perched on bedrock (Fig. 2B) provide a constraint on the interpretation of the bedrock ^{10}Be ages. They both concur that Hunt Bluff was deglaciaded by the early Holocene; it follows that the site was ice-covered for several thousand years prior to that, and therefore the bedrock ^{10}Be ages cannot represent continuous exposure of Hunt Bluff since the last interglacial period.

This leads to the question of whether Hunt Bluff was glaciaded at the LGM. The extent and thickness of the Antarctic Ice Sheet during the LGM is important for providing reliable estimates of the maximum ice sheet volume and loading during the last glacial period, which are in turn needed for tuning ice sheet and Glacial Isostatic Adjustment models that are used to predict the likely contribution from various sectors of Antarctica to future sea level rise (Bentley, 2010). Knowing whether sites along the Amundsen Sea coast were exposed during the LGM is important for providing constraints on the surface profile of the WAIS in this region (Larter et al., 2014). Furthermore, biologists are presently searching for locations in Antarctica where organisms could have persisted through multiple glacial cycles, evidence for which is necessary to explain the observed biogeographic distribution of fauna. Such locations are likely to be nunataks that were not ice-covered during the LGM (Convey et al., 2009). Evidence for continuous exposure of coastal hills through more than one glacial cycle has been identified elsewhere in Antarctica even where the ice sheet had thickened and extended onto the continental shelf during the LGM (e.g. Larsemann Hills, Hodgson et al., 2001; Bunge Hills, Gore et al., 2001). In those cases, localized drawdown occurred and ice was preferentially discharged to the ocean/ice shelves through outlet glaciers. In a similar manner, it is feasible that ice flow through the adjacent Zuniga and True Glaciers (Fig. 2) could have kept Hunt Bluff ice-free during the LGM when the WAIS was more extensive (Larter et al., 2014).

Since the ^{10}Be ages do not indicate when the last phase of ice cover began, we employed a multi-nuclide approach to determine if the site was ice-covered during the LGM. Here the global LGM

(19–26.5 ka; Clark et al., 2009) is used in order to avoid confusion resulting from the fact that different parts of the Antarctic ice sheet reached their last maximum extent at different times (Stone et al., 2003; RAISED Consortium, 2014). The calculations described in section 5.3 suggest that at least a few tens of metres of ice – the minimum required to stop ^{10}Be and ^{14}C production in the bedrock – was present on Hunt Bluff from 21.1 ± 5.8 ka (i.e. potentially between 15.3 and 26.9 ka) until 9.6 ka. 71% of the realizations in the uncertainty analysis were younger than 22.4 ka (Fig. 3A), which is consistent with onset of the final glaciation most likely occurring during the latter part of LGM (Fig. 3B). Whilst there could have been thinner ice present prior to the time calculated for onset of ice cover, it could not have been more than a few tens of metres thick. This implies that thickening sufficient to cover the site occurred rapidly, rather than over a period of several thousand years. In the much less likely scenario that glaciation started prior to 22.4 ka, Hunt Bluff may not have been ice-free during much, if any, of the LGM period. In summary, the new *in situ* ^{14}C data suggest that Hunt Bluff was most likely not ice-free for all of the LGM.

Whilst the ^{10}Be data imply that Hunt Bluff was exposed during multiple interglacials, they cannot provide evidence for timing and/or duration of exposure prior to the last glacial period. Pairing ^{10}Be – ^{26}Al cannot identify intermittent exposures over multiple glacial cycles in the Hunt Bluff samples because only periods of ice cover of more than 100 kyrs can be reliably detected, and the ^{10}Be exposure ages are not much greater than that. Furthermore, the bedrock $^{14}\text{C}/^{10}\text{Be}$ ratio does not detect fluctuations in ice cover prior to ~30 ka (cf. White et al., 2011; Briner et al., 2014; Fogwill et al., 2014; Balco et al., 2016). The alternative is a simple calculation of minimum total history based on the cumulative total of likely ice-free periods and the corresponding bedrock ^{10}Be exposure ages (cf. Fabel et al., 2002). However, since the results of our study do not preclude that Hunt Bluff was ice-free during the early part of the LGM (Fig. 3B), we cannot assume that the site was ice-free only during interglacials, and are therefore not able to use this approach.

8. Wider implications

8.1. The last glaciation in the central Amundsen Sea Embayment

8.1.1. Ice sheet thickness and extent

Results of the ^{10}Be and ^{14}C analyses suggest that Hunt Bluff was covered by thick ice at least once since the last interglacial period, and that the last occupation most likely lasted from sometime around 21.1 ka to 9.6 ka (Fig. 3B). The data imply that the ice surface must have been at least 420 m above present in the central

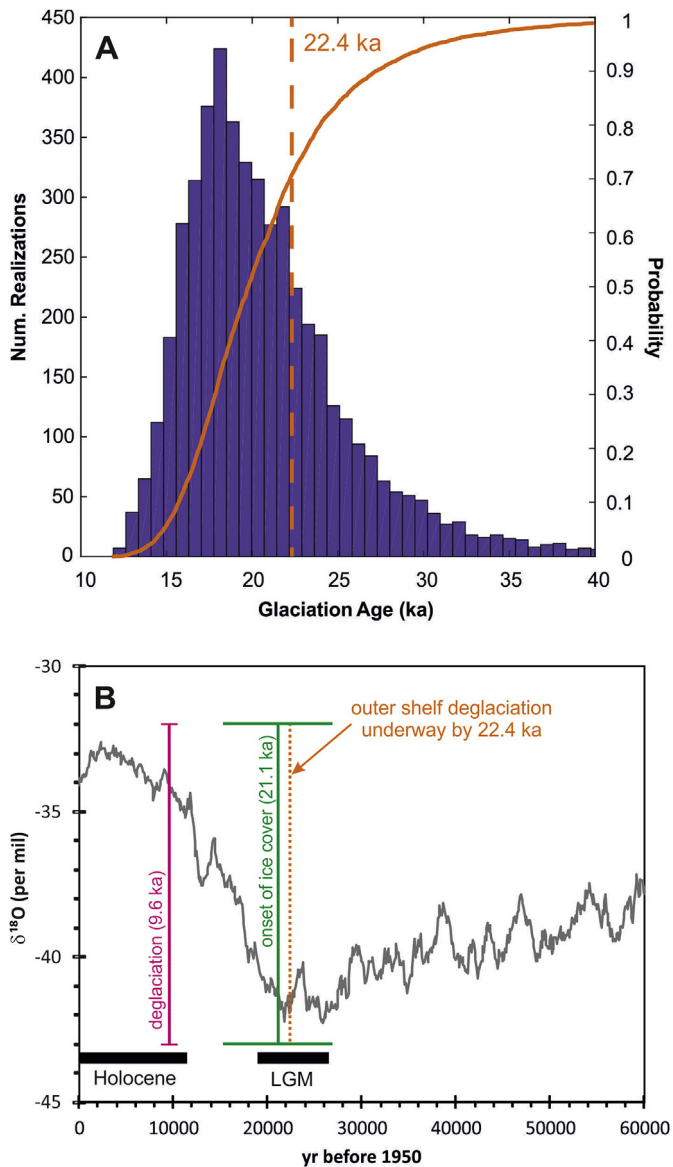


Fig. 3. Timing of the last glaciation at Hunt Bluff. A. Estimated times for the onset of ice cover, derived from a Monte Carlo simulation (see text). The mean and standard deviation of all 5000 realizations – representing the most likely timing of onset of glaciation – is 21.1 ± 5.8 ka. The solid yellow line is a cumulative distribution curve. The yellow dashed line marks the timing of retreat of grounded ice from the edge of the continental shelf in the western ASE (Smith et al., 2011). B. Duration of glacial cover at Hunt Bluff in relation to the $\delta^{18}\text{O}$ temperature record (plotted on the WDC2014 timescale; WAIS Divide project members, 2013, 2015; Fudge et al., 2016) from the nearest ice core to Hunt Bluff, WAIS Divide ice core, which is situated 550 km to the south. The black horizontal bars denote the duration of the Holocene epoch, and the global LGM (Clark et al., 2009). All uncertainties shown are 1σ . (For interpretation of the references to colour in this figure legend, the reader is referred to the web version of this article.)

Amundsen Sea Embayment during the last glaciation in order to cover our bedrock samples and deposit the erratic cobble BR-02 at Hunt Bluff. Bear Peninsula was therefore probably not a refugium for biological organisms during the LGM (Convey et al., 2009) because thick ice cover for at least part of that period would have prevented their survival. The ice sheet thickness derived from our exposure dating is consistent with records from other nunataks in the ASE (Mount Murphy and the Hudson Mountains; Johnson et al.,

2008, 2014) that suggest ice was at least 150–330 m thicker than present at the glacial maximum (moreover, if lower global mean sea level at LGM is taken into account, these values are around 120 m higher; Peltier and Fairbanks, 2006). Whilst records of ice sheet thickness from across the wider Amundsen Sea sector are relatively sparse, ice more than 400 m thicker than today was also present during the last glaciation at the westernmost margin of the Ford Ranges (Stone et al., 2003; Larter et al., 2014), 900 km west of Bear Peninsula.

The profile of an ice sheet margin is important because it affects the dynamics of ice flow (Mackintosh et al., 2011; Larter et al., 2014), which has implications for ice sheet models that incorporate such flow dynamics. However, since the WAIS is thought to have extended to the continental shelf break at the northernmost extent of the Dotson-Getz Trough (Smith et al., 2011) and in most other parts of the Amundsen Sea Embayment (Larter et al., 2014) at the LGM, and since our results show that Hunt Bluff was probably ice-covered at some point during that time, it is unlikely that the surface gradient of the WAIS was particularly low in this region.

8.1.2. Comparison with marine evidence for timing of grounded ice-cover

Marine sediment core data suggest that retreat of grounded ice from the continental shelf edge was underway by 22.4 cal kyr BP (Smith et al., 2011). Our uncertainty analysis implies a 71% chance that glaciation at Hunt Bluff started after 22.4 ka (Fig. 3A). Thus, it is likely that the onset of glaciation at Hunt Bluff post-dated the maximum extent of grounded ice on the nearby continental shelf (i.e. the time when the grounding line was located at or near the shelf edge). Such thickening when retreat was already underway may seem contradictory, but evidence from the Ross Sea sector shows that such a situation is not unique: at Mount Waesche and in the Ohio Range, in the interior of Marie Byrd Land, maximum ice sheet thicknesses did not occur during glacial maxima, implying that ice surface elevation did not fluctuate in phase with changes in ice sheet extent (Ackert et al., 2013). Indeed, the maximum thicknesses at Mount Waesche and in the Ohio Range during the last glacial period occurred at 10–12 ka (Ackert et al., 2013), while grounding line retreat from the outer Ross Sea shelf started before c. 13 cal. kyr BP (Anderson et al., 2014). We envisage that near-simultaneous ice sheet thickening and grounding line retreat was caused by grounding of ice shelves in the deep inner shelf basins of the Dotson-Getz Trough (Fig. 4). We suggest that at the beginning of the last glacial period the Dotson Ice Shelf, and the Getz A and Getz B ice shelves, advanced northwards and re-grounded on the shallow middle continental shelf north of the deep inner shelf basins, thereby creating a subglacial lake setting in those basins (cf. Aley et al., 2006). Grounded ice flowed unconfined as a sheet across the middle and outer shelf to near the shelf break (Fig. 4A). At the LGM, the floating parts of this sheet thickened and grounded in the inner shelf basins (cf. Palmer Deep; Domack et al., 2006), resulting in (i) re-organisation of grounded ice flow on the inner continental shelf, with convergence of the Dotson and Getz A and B tributaries and development of the Dotson-Getz palaeo-ice stream, and (ii) damming-up of ice in the Dotson tributary resulting in thickening of ice at Hunt Bluff.

This scenario is consistent with the submarine geomorphology immediately offshore from the Dotson and Getz ice shelves. Ice formerly flowed from the coast of the central and western ASE across the continental shelf in three palaeo-ice stream troughs that were connected on the mid-shelf (Larter et al., 2009). Two distinct sets of subglacial lineations with differing orientations (Fig. 4A and B) have been mapped within the Dotson-Getz palaeo-ice stream trough and on shallow banks to the east and west of the trough (Graham et al., 2009). The NNW-oriented lineations on the bank to

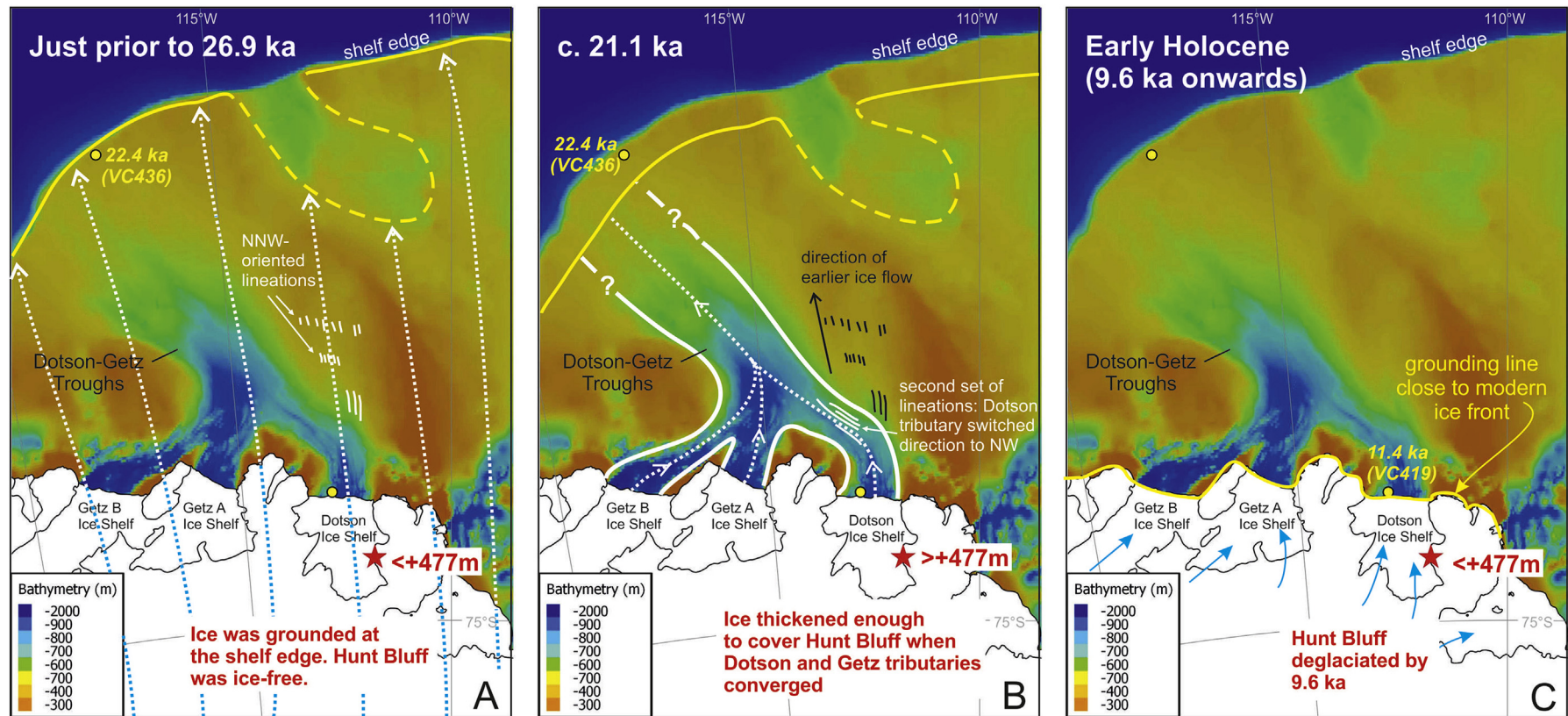


Fig. 4. Schematic diagram (panels A–C) illustrating a mechanism for thickening of ice at Hunt Bluff around 21.1 ka, with subsequent deglaciation by the early Holocene. The red star denotes the location of our study site at Hunt Bluff on Bear Peninsula; ice thicknesses derived from this study are shown adjacent to this on each panel. Regional bathymetry is from Arndt et al. (2013). The solid black line represents the modern coastline, with ice shelves labelled. The approximate position of the grounding line (taken from Larter et al., 2014) is indicated by a yellow line; where dashed, this indicates uncertainty in its position. Yellow circles indicate the locations of marine sediment cores mentioned in the text, with associated core IDs and calibrated radiocarbon dates for retreat of grounded ice. Possible ice flow paths are shown as white/blue dotted lines. A. Ice sheet configuration immediately prior to the time when ice became thick enough to cover Hunt Bluff, for which the earliest possible date is 26.9 ka. At this time, grounded ice flowed as a sheet to, or near to, the shelf edge (Larter et al., 2014), while ice shelf conditions prevailed within the tributary troughs. Subglacial lineations (Graham et al., 2009; lines shown here are approximate representations of their data) on the eastern bank of the Dotson-Getz palaeo ice-stream trough suggest flow across the continental shelf in a NNW direction. The ice sheet had not yet thickened enough to cover Hunt Bluff. B. Ice sheet configuration c. 21.1 ka (around the LGM). The grounding line had retreated from the shelf edge by 22.4 cal kyr BP (constrained by core VC436; Smith et al., 2011). Exposure dating indicates that ice had thickened sufficiently to cover Hunt Bluff sometime between 15.3 and 26.9 ka, with 21.1 ka as the most likely time for this. A second set of subglacial lineations within the Dotson-Getz palaeo ice-stream trough and its inner shelf tributaries (Graham et al., 2009) suggests that flow re-organisation occurred, probably due to the grounding of the ice in the inner shelf basins and onset of topographic control of ice flow, resulting in a switch from earlier flow in a NNW-direction to a north-westerly direction, convergence of ice flow from the Dotson and Getz tributaries and thickening of ice at Hunt Bluff. C. Ice sheet configuration by the early Holocene. Exposure dating in this study revealed that Hunt Bluff had completely deglaciated by 9.6 ka, coincident or very shortly after retreat of grounded ice close to the modern Dotson Ice Shelf front by 11.4 cal kyr BP (constrained by core VC419; Smith et al., 2011). Radiocarbon dates from marine sediment cores in front of the Getz A and B ice shelves suggest the grounding line had retreated close to their modern fronts around the same time (Smith et al., 2011; Hillenbrand et al., 2013). Blue arrows indicate modern ice flow directions. (For interpretation of the references to colour in this figure legend, the reader is referred to the web version of this article.)

the east of the Dotson-Getz Trough were likely associated with grounded ice that flowed in a sheet-like manner to the continental shelf edge (Fig. 4A). According to Graham et al. (2009), this set of lineations formed prior to or during an early phase of the last glacial period. We suggest that the date of 22.4 cal kyr BP obtained from a marine sediment core on the outermost shelf of the western ASE (Fig. 4A and B) marks the end of this phase of sheet-like ice flow. The second set of lineations, oriented NW-SE within the Dotson trough, provide evidence for a later change in flow direction. This change in flow direction may have been caused by grounding of ice in the inner-shelf basins, resulting in topographic control of ice flow. This would have led in turn to the merging of the Dotson and Getz A and B ice stream tributaries to form a single large palaeo-ice stream that drained through the main Dotson-Getz Trough onto the middle- and outer-shelf (Larter et al., 2009) but did not reach the shelf edge (Fig. 4B). We envisage that the inner shelf grounding and convergence of flow effectively impeded the flow of ice in the Dotson tributary, causing it to “dam up”, resulting in ice thickening at Hunt Bluff. If this mechanism is correct, then the age for onset of ice cover at Hunt Bluff (21.1 ± 5.8 ka) provides a minimum date for the flow-switch, i.e. the change in ice flow direction must have occurred just prior to glaciation at Hunt Bluff. Similar flow re-organisation during the last deglaciation, involving a change from unconfined ice sheet flow to topographically-confined flow, has been inferred from subglacial bedforms in Canada (Ó Cofaigh et al., 2010).

Modelling by Colledge et al. (2013) reconstructed LGM flow routes that appear to preferentially divert ice around Bear Peninsula whilst flow is focused through the Dotson tributary (their Fig. 4A). If correct, such a pattern of ice flow would have resulted in Hunt Bluff being exposed, rather than ice-covered, for at least the LGM. However, according to the present study, maximum ice sheet thickening at Hunt Bluff occurred between 27 and 15 ka, i.e. during, or towards the end of, the LGM. This persisted only until the Dotson-Getz palaeo-ice stream started to retreat from the outer shelf, which would have brought about a rapid drawdown of ice, eventually exposing Hunt Bluff again (Fig. 4C).

An alternative to the scenario described above is stagnation (i.e. “switching-off”) of northward flow from Kohler Glacier. This would also have resulted in thickening of ice at Hunt Bluff. A similar situation is found at the Kamb Ice Stream on the Siple Coast of Antarctica today: the ice stream is currently thickening, following stagnation ~150 years ago (Anandkrishnan and Alley, 1997; Joughin and Tulaczyk, 2002; Pritchard et al., 2009). Given the present rate of thickening of Kamb Ice Stream (~ 0.45 m yr⁻¹; Pritchard et al., 2009), it would take only 950 years for grounded ice with a surface at the altitude of the present surface of the Dotson Ice Shelf to thicken enough to cover Hunt Bluff. However, studies of the clay mineral compositions in diamictons from sediment cores recovered from the middle- and outer-shelf parts of the Dotson-Getz trough (i.e. north of the convergence of the Dotson and Getz tributaries) did not find a change in provenance (Ehrmann et al., 2011; Smith et al., 2011). This implies that the source of clay minerals delivered to those sediments did not change, and therefore that both the Dotson and Getz tributaries continuously supplied detritus to the core sites during the later stage of the last glacial period. We therefore favour a mechanism of flow re-organisation in which the Dotson and Getz tributaries grounded in the inner shelf basins and merged to form the Dotson-Getz palaeo-ice stream around 21.1 ka (Fig. 4B).

8.2. Comparison with ice sheet models

Glacio-geological data such as exposure ages are essential for validating models that are used to predict future contribution of the

Antarctic ice sheet to sea level rise. Fig. 5 shows reconstructions of ice sheet thickness (relative to present) from three ice sheet models. The model grid points used to produce the results shown are located over Hunt Bluff; however, the model resolutions are such that there is no difference in output if the grid points were to be located over the Dotson Ice Shelf (Colledge et al., 2014; is based on a 15×15 km grid, whereas both Pollard et al., 2016; Whitehouse et al., 2012, use a 20×20 km grid). None of the models have resolutions high enough to resolve localized effects, thus they can only provide a regional picture of ice sheet change. Nevertheless, some observations can be made:

- All three models suggest that Hunt Bluff was ice-covered for all of the LGM period, and predict significant thinning of the WAIS following the LGM, with up to 970 m thickness of ice lost (of the three models, Pollard et al., 2016 predicts the lowest ice loss: 720 m). However, the thickness of ice cover over Hunt Bluff during the LGM varies: Pollard et al. (2016) predicts that the ice sheet was at least 240 m thicker than present for the whole LGM. Whitehouse et al. (2012) suggests that ice may have been up to 490 m thicker at 20 ka, but does not provide thicknesses for other times during the LGM period. Colledge et al. (2014) predicts that ice sheet thickness fluctuated significantly during the LGM, but that Hunt Bluff was never completely deglaciated until after that time.
- The style of post-LGM thinning varies between the models, but there is broad agreement in the timing: Whitehouse et al. (2012) predicts thinning between 20 and 5 ka (the temporal resolution of the model output is not high enough to determine whether this was steady), Pollard et al. (2016) predicts steady and progressive thinning between 15 and 6 ka, and Colledge et al. (2014) shows an overall thinning trend between 19 and 7 ka, but with several fluctuations in ice thickness.
- The models all suggest that Hunt Bluff has remained ice-free since just prior to the Holocene (by ~15 ka for Colledge et al., 2014; Whitehouse et al., 2012, and by ~12.5 ka for Pollard et al., 2016). These predictions are at least 3000 years earlier

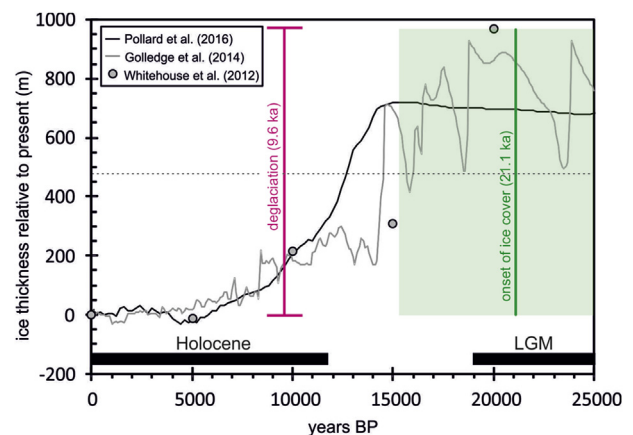


Fig. 5. Model predictions for ice sheet thickness since LGM over Bear Peninsula. Output from three models is shown (Pollard et al., 2016; Colledge et al., 2014; Whitehouse et al., 2012). The dotted line shows the elevation of Hunt Bluff, and therefore the thickness of ice above which the sample sites would be ice-covered. The magenta line represents the deglaciation age we obtained for Hunt Bluff (9.6 ± 0.9 ka), determined by ¹⁴C analysis of erratic cobble BR-02. The green line represents the time when ice cover at Hunt Bluff became sufficiently thick to stop production of cosmogenic isotopes in the bedrock (mean age 21.1 ± 5.8 ka from our calculations). 1σ uncertainties are indicated by green shading. The black horizontal bars denote the duration of the Holocene epoch, and the global LGM (Clark et al., 2009). (For interpretation of the references to colour in this figure legend, the reader is referred to the web version of this article.)

than our exposure age data suggest. The Golledge et al. (2014) model output additionally suggests a complete, but short-lived (~400 yr-long) deglaciation of Hunt Bluff just after 16 ka. If real, this implies that the ice sheet surface could not have thinned much below the bedrock elevation of Hunt Bluff during the period when it was deglaciated. Such short-lived periods of exposure would, however, not be detectable using exposure dating.

- None of the models predict the onset of glaciation after 25 ka, and they are unable to provide information about ice sheet thickness prior to that because either their initial states used grids of lower resolution (e.g. Pollard et al., 2016) or they were originally designed for a different purpose (e.g. Whitehouse et al., 2012 was intended for reproducing ice sheet configuration under LGM conditions, rather than predicting ice sheet change through time). However, the results of this study imply that Hunt Bluff became glaciated at some time during the LGM, with a strong likelihood that the onset of that glaciation was later than 22.4 ka. A possible reason for this and other inconsistencies is that the models have relatively coarse resolutions, and the thinning history of Hunt Bluff may not be representative of the wider region.

In summary, the models are in reasonable agreement about the magnitude and timing of deglaciation of Hunt Bluff, but predict deglaciation at least 3000 years earlier than suggested by our results. The onset of glaciation suggested by our data is not predicted by the models; further studies with higher-resolution and longer model runs are needed to study the initiation of the last glaciation.

9. Conclusions

New ^{10}Be and *in situ* ^{14}C exposure age data suggest that the onset of the last ice overriding at Bear Peninsula began between 26.9 and 15.3 ka (the most likely time around 21.1 ka), and lasted until 9.6 ka. These results imply that deglaciation occurred concurrently with other sites across the ASE. The data also suggest that Hunt Bluff last became covered by the West Antarctic Ice Sheet (WAIS) at some point during the LGM, potentially by means of flow re-organisation resulting in the convergence of the Dotson and Getz palaeo-ice streams. It is therefore unlikely to have acted as a biological refugium during the last glacial period. The range of bedrock ^{10}Be ages (118–144 ka) obtained from the study site imply that it experienced repeated exposure and burial by the WAIS prior to the last period of ice cover, but they do not permit estimation of the total history required.

This study provides terrestrial constraints on the timing of onset of the last glaciation of Bear Peninsula. High-resolution and longer model runs extending beyond 25 ka are needed in order to study the initiation of glaciation across the wider region. Future investigations should also seek to address the severe lack of glacial-geological data, which are required for validating and improving ice sheet models, by collecting geomorphological data and samples for exposure dating from exposed bedrock sites adjacent to the main ice streams draining the central Amundsen Sea Embayment (Smith, Pope and Kohler Glaciers). This need is demonstrated by the inability of three well-known models to reliably reproduce the timing of the final deglaciation of Hunt Bluff inferred from our exposure age dating.

Acknowledgements

We thank the Captain, crew and helicopter pilots of RV Polarstern cruise ANT-XXVI/3 for their logistical support, and British Antarctic Survey field assistant Ian McNab for assisting with

fieldwork. Technical support was provided by Mike Tabecki and Hilary Blagbrough (BAS), and Roseanne Schwartz and Jean Hanley (LDEO). Laura Gerrish (BAS Mapping & Geographic Information Unit) helped with preparing Fig. 1. We thank Dominic Hodgson, Kelly Hogan, Rob Larter, and Eric Wolff for useful discussions, and Nick Golledge, David Pollard and Pippa Whitehouse for providing the model outputs for Fig. 5. Greg Balco and an anonymous reviewer provided thorough and constructive comments which significantly improved the manuscript. JSJ acknowledges the support of Natural Environment Research Council (NERC) grant NE/K012088/1. This work forms part of the British Antarctic Survey 'Polar Science for Planet Earth' programme, also funded by NERC.

Appendix A. Supplementary data

Supplementary data related to this article can be found at <https://doi.org/10.1016/j.quascirev.2017.11.003>.

References

- Ackert, R.P., Putnam, A.E., Mukhopadhyay, S., Pollard, D., DeConto, R.M., Kurz, M.D., Borns, H.W., 2013. Controls on interior West Antarctic Ice Sheet Elevations: inferences from geologic constraints and ice sheet modelling. *Quat. Sci. Rev.* 65, 26–38.
- Alley, R.B., Dupont, T.K., Parizek, B.R., Anandakrishnan, S., Lawson, D.E., Larson, G.J., Evenson, E.B., 2006. Outburst flooding and the initiation of ice-stream surges in response to climatic cooling: a hypothesis. *Geomorphology* 75, 76–89.
- Alley, R.B., Anandakrishnan, S., Christianson, K., Horgan, H.J., Muto, A., Parizek, B.R., Pollard, D., Walker, R.T., 2015. Ocean forcing of ice-sheet retreat: West Antarctica and more. *Annu. Rev. Earth Pl. Sc.* 43, 7.1–7.25. <https://doi.org/10.1146/annurev-earth-060614-105344>.
- Anandakrishnan, S., Alley, R.B., 1997. Stagnation of ice stream C, West Antarctica by water piracy. *Geophys. Res. Lett.* 24, 265–268.
- Anderson, J.B., Conway, H., Bart, P.J., Witus, A.E., Greenwood, S.L., McKay, R.M., Hall, B.L., Ackert, R.P., Licht, K., Jakobsson, M., Stone, J.O., 2014. Ross Sea paleo-ice sheet drainage and deglacial history during and since the LGM. *Quat. Sci. Rev.* 100, 31–54.
- Arndt, J.E., Schenke, H.W., Jakobsson, M., Nitsche, F.O., Buys, G., Golby, B., Resbeco, M., Bohoyo, F., Hong, J.K., Black, J., Greku, R.K., Udintsev, G.B., Barrios, F., Peralta-Reynoso, W., Taisei, M., Wigley, R., 2013. The International Bathymetric Chart of the Southern Ocean Version 1.0 - a new bathymetric compilation covering circum-Antarctic waters. *Geophys. Res. Lett.* 40 (9), 1–7.
- Arthern, R.J., Winebrenner, D.P., Vaughan, D.G., 2006. Antarctic snow accumulation mapped using polarization of 4.3-cm wavelength microwave emission. *J. Geophys. Res.* 111, D06107.
- Balco, G., Stone, J.O., Lifton, N.A., Dunai, T.J., 2008. A complete and easily accessible means of calculating surface exposure ages or erosion rates from ^{10}Be and ^{26}Al measurements. *Quat. Geochronol.* 3, 174–195.
- Balco, G., 2011. Contributions and unrealized potential contributions of cosmogenic-nuclide exposure dating to glacier chronology, 1990–2010. *Quat. Sci. Rev.* 30, 3–27.
- Balco, G., Todd, C., Huybers, K., Campbell, S., Vermeulen, M., Hegland, M., Goehring, B.M., Hillebrand, T.M., 2016. Cosmogenic nuclide exposure ages from the Pensacola Mountains adjacent to the Foundation Ice Stream, Antarctica. *Am. J. Sci.* 316, 542–577.
- Bentley, M.J., 2010. The Antarctic palaeo record and its role in improving predictions of future Antarctic Ice Sheet change. *J. Quat. Sci.* 25, 5–18.
- Bentley, M.J., Fogwill, C.J., LeBrocq, A.M., Hubbard, A.L., Sugden, D.E., Dunai, T.J., Freeman, S.P.H.T., 2010. Deglacial history of the West Antarctic Ice Sheet in the Weddell Sea embayment: constraints on past ice volume change. *Geology* 38, 411–414.
- Bierman, P.R., Marsella, K.A., Patterson, C., Davis, P.T., Caffee, M., 1999. Mid-Pleistocene cosmogenic minimum-age limits for pre-Wisconsinan glacial surfaces in southwestern Minnesota and southern Baffin Island: a multiple nuclide approach. *Geomorphology* 27, 25–39.
- Briggs, R.D., Tarasov, L., 2013. How to evaluate model-derived deglaciation chronologies: a case study using Antarctica. *Quat. Sci. Rev.* 63, 109–127.
- Briner, J.P., Lifton, N.A., Miller, G.H., Refsnider, K., Anderson, R., Finkel, R., 2014. Using *in situ* cosmogenic ^{10}Be , ^{14}C , and ^{26}Al to decipher the history of polythermal ice sheets on Baffin Island, Arctic Canada. *Quat. Geochronol.* 19, 4–13.
- Chmeleff, J., von Blanckenburg, F., Kossert, K., Jakob, D., 2010. Determination of the Be-10 half-life by multicollector ICP-MS and liquid scintillation counting. *Nucl. Instrum. Methods Phys. Res. B* 268, 192–199.
- Clark, P.U., Dyke, A.S., Shakun, J.D., Carlson, A.E., Clark, J., Wohlfarth, B., Mitrovica, J.X., Hostetler, S.W., McCabe, A.M., 2009. The Last Glacial Maximum. *Science* 325, 710–714.
- Convey, P., Stevens, M.I., Hodgson, D.A., Smellie, J.L., Hillenbrand, C.-D., Barnes, D.K.A., Clarke, A., Pugh, P.J.A., Linse, K., Cary, S.C., 2009. Exploring biological constraints on the glacial history of Antarctica. *Quat. Sci. Rev.* 28,

- 3035–3048.
- Domack, E., Amblàs, D., Gilbert, R., Brachfeld, S., Camerlenghi, A., Rebesco, M., Canals, M., Urgeles, R., 2006. Subglacial morphology and glacial evolution of the Palmer deep outlet system, Antarctic Peninsula. *Geomorphology* 75, 125–142.
- Ehrmann, W., Hillenbrand, C.-D., Smith, J.A., Graham, A.G.C., Kuhn, G., Larter, R., 2011. Provenance changes between recent and glacial-time sediments in the Amundsen Sea embayment, West Antarctica: clay mineral assemblage evidence. *Antarct. Sci.* 23, 471–486.
- Emslie, S.D., Coats, L., Licht, K., 2007. A 45,000 yr record of Adélie penguins and climate change in the Ross Sea, Antarctica. *Geology* 35, 61–64.
- Fabel, D., Stroeven, A.P., Harbor, J., Kleman, J., Elmore, D., Fink, D., 2002. Landscape preservation under Fennoscandian ice sheets determined from *in situ* produced ^{10}Be and ^{26}Al . *Earth Planet. Sc. Lett.* 201, 397–406.
- Fogwill, C.J., Turney, C.S.M., Gollidge, N.R., Rood, D.H., Hippe, K., Wacker, L., Wieler, R., Rainsley, E.B., Jones, R.S., 2014. Drivers of abrupt Holocene shifts in West Antarctic ice stream direction determined from combined ice sheet modelling and geologic signatures. *Antarct. Sci.* 26 (6), 674–686.
- Fretwell, P., et al., 2013. BEDMAP2: improved ice bed, surface and thickness datasets for Antarctica. *Cryosphere* 7, 375–393.
- Fudge, T.J., Markle, B.R., Cuffey, K.M., Buizert, C., Taylor, K.C., Steig, E.J., Waddington, E.D., Conway, H., Koutnik, M., 2016. Variable relationship between accumulation and temperature in West Antarctica for the past 31,000 years. *Geophys. Res. Lett.* 43, 3795–3803.
- Goehring, B.M., Schaefer, J.M., Schluechter, C., Lifton, N.A., Finkel, R.C., Jull, A.J.T., Akçar, N., Alley, R.B., 2011. The Rhone Glacier was smaller than today for most of the Holocene. *Geology* 39, 679–682.
- Goehring, B.M., Schimmelpennig, I., Schaefer, J.M., 2014. Capabilities of the Lamont-Doherty Earth Observatory *in situ* ^{14}C extraction laboratory updated. *Quat. Geochronol.* 19, 194–197.
- Gollidge, N.R., Levy, R.H., McKay, R.M., Fogwill, C.J., White, D.A., Graham, A.G.C., Smith, J.A., Hillenbrand, C.-D., Licht, K.J., Denton, G.H., Ackert, R.P., Maas, S.M., Hall, B.L., 2013. Glaciology and geological signature of the Last Glacial Maximum Antarctic ice sheet. *Quat. Sci. Rev.* 78, 225–247.
- Gollidge, N.R., Menviel, L., Carter, L., Fogwill, C.J., England, M.H., Cortese, G., Levy, R.H., 2014. Antarctic contribution to meltwater pulse 1A from reduced Southern Ocean overturning. *Nat. Commun.* 5, 5107. <https://doi.org/10.1038/ncomms6107>.
- Gore, D.B., Rhodes, E.J., Augustinus, P.C., Leishman, M.R., Colhoun, E.A., Rees-Jones, J., 2001. Rhone Hills, East Antarctica: ice free at the Last Glacial Maximum. *Geology* 29, 1103–1106.
- Graham, A.G.C., Larter, R.D., Gohl, K., Hillenbrand, C.-D., Smith, J.A., Kuhn, G., 2009. Bedform signature of a West Antarctic palaeo-ice stream reveals a multi-temporal record of flow and substrate control. *Quat. Sci. Rev.* 28, 2774–2793.
- Graham, A.G.C., Larter, R.D., Gohl, K., Dowdeswell, J.A., Hillenbrand, C.-D., Smith, J.A., Evans, J., Kuhn, G., Deen, T., 2010. Flow and retreat of the Late Quaternary Pine Island-Thwaites palaeo-ice stream, West Antarctica. *J. Geophys. Res.* 115, F03025.
- Hein, A.S., Fogwill, C.J., Sugden, D.E., Xu, S., 2011. Glacial/interglacial ice-stream stability in the Weddell Sea embayment, Antarctica. *Earth Planet. Sc. Lett.* 307, 211–221.
- Hillenbrand, C.-D., Kuhn, G., Smith, J.A., Gohl, K., Graham, A.G.C., Larter, R.D., Klages, J.P., Downey, R., Moreton, S.G., Forwick, M., Vaughan, D.G., 2013. Grounding-line retreat of the west Antarctic ice sheet from inner Pine Island Bay. *Geology* 41, 35–38.
- Hodgson, D.A., Noon, P.E., Vyverman, W., Bryant, C.L., Gore, D.B., Appleby, P., Gilmour, M., Verleyen, E., Sabbe, K., Jones, V.J., Ellis-Evans, J.C., Wood, P.B., 2001. Were the Larsemann Hills ice-free through the Last Glacial Maximum? *Antarct. Sci.* 13, 440–454.
- Johnson, J.S., Bentley, M.J., Gohl, K., 2008. First exposure ages from the Amundsen Sea Embayment, West Antarctica: the Late Quaternary context for recent thinning of Pine Island, Smith, and Pope Glaciers. *Geology* 36 (3), 223–226.
- Johnson, J.S., Bentley, M.J., Smith, J.A., Finkel, R.C., Rood, D.H., Gohl, K., Balco, G., Larter, R.D., Schaefer, J.M., 2014. Rapid thinning of Pine Island Glacier in the early Holocene. *Science* 343, 999–1001.
- Joughin, I., Alley, R.B., 2011. Stability of the West Antarctic Ice Sheet in a warming world. *Nat. Geosci.* 4, 506–513.
- Joughin, I., Tulaczyk, S., 2002. Positive mass balance of the Ross ice streams, West Antarctica. *Science* 295, 476–280.
- Jull, A.J.T., Scott, E.M., Bierman, P., 2015. The CRONUS-Earth inter-comparison for cosmogenic isotope analysis. *Quat. Geochronol.* 26, 3–10.
- King, M.A., Bingham, R.J., Moore, P., Whitehouse, P.L., Bentley, M.J., Milne, G.A., 2012. Lower satellite-gravimetry estimates of Antarctic sea-level contribution. *Nature* 491, 586–590.
- Kirshner, A., Anderson, J.B., Jakobsson, M., O'Regan, M., Majewski, W., Nitsche, F., 2012. Post-LGM deglaciation in Pine Island Bay, west Antarctica. *Quat. Sci. Rev.* 38, 11–26.
- Korschinek, G., Bergmaier, A., Faestermann, T., Gerstmann, U.C., Knie, K., Rugal, G., Wallner, A., Dillmann, I., Dollinger, G., Liese von Gostomski, C., Kossert, K., Maiti, M., Poutivtsev, M., Rimmert, A., 2010. A new value for the half-life of Be-10 by heavy-ion elastic recoil detection and liquid scintillation counting. *Nucl. Instrum. Methods Phys. Res. B* 268, 187–191.
- Lal, D., 1991. Cosmic ray labeling of erosion surfaces: *in situ* nuclide production rates and erosion models. *Earth Planet. Sc. Lett.* 104, 424–439.
- Larter, R.D., Graham, A.G.C., Gohl, K., Kuhn, G., Hillenbrand, C.-D., Smith, J.A., Deen, T.J., Livermore, R.A., Schenke, H.-W., 2009. Subglacial bedforms reveal complex basal regime in a zone of paleo-ice stream convergence, Amundsen Sea Embayment, West Antarctica. *Geology* 37, 411–414.
- Larter, R.D., Anderson, J.B., Graham, A.G.C., Gohl, K., Hillenbrand, C.-D., Jakobsson, M., Johnson, J.S., Kuhn, G., Nitsche, F.O., Smith, J.A., Witus, A.E., Bentley, M.J., Dowdeswell, J.A., Ehrmann, W., Klages, J.P., Lindow, J., O Cofaigh, C., Spiegel, C., 2014. Reconstruction of changes in the Amundsen Sea and Bellingshausen Sea sector of the West Antarctic Ice Sheet since the Last Glacial Maximum. *Quat. Sci. Rev.* 100, 55–86.
- Lifton, N.A., Sato, T., Dunai, T.J., 2014. Scaling *in situ* cosmogenic nuclide production rates using analytical approximations to atmospheric cosmic-ray fluxes. *Earth Planet. Sc. Lett.* 386, 149–160.
- Lilly, K., Fink, D., Fabel, D., Lambeck, K., 2010. Pleistocene dynamics of the interior East Antarctic ice sheet. *Geology* 38, 703–706.
- Lindow, J., Castex, M., Wittmann, H., Johnson, J.S., Lisker, F., Gohl, K., Spiegel, C., 2014. Glacial retreat in the Amundsen Sea sector, West Antarctica – first cosmogenic evidence from central Pine Island Bay and the Kohler Range. *Quat. Sci. Rev.* 98, 166–173.
- Lisiecki, L.E., Raymo, M.E., 2005. A Pliocene-Pleistocene stack of 57 globally distributed benthic d^{18}O records. *Paleoceanography* 20, PA1003.
- Mackintosh, A., White, D., Fink, D., Gore, D.B., Pickard, J., Fanning, P.C., 2007. Exposure ages from mountain dipsticks in Mac. Robertson Land, East Antarctica, indicate little change in ice-sheet thickness since the Last Glacial Maximum. *Geology* 35, 551–554.
- Mackintosh, A., Gollidge, N., Domack, E., Dunbar, R., Leventer, A., White, D., Pollard, D., DeConto, R., Fink, D., Zwart, D., Gore, D., Lavoie, C., 2011. Retreat of the East Antarctic ice sheet during the last glacial termination. *Nat. Geosci.* 4, 195–202.
- Miller, G., Briner, J., Lifton, N., Finkel, R., 2006. Limited ice-sheet erosion and complex exposure histories derived from *in situ* cosmogenic ^{10}Be , ^{26}Al , and ^{14}C on Baffin Island, Arctic Canada. *Quat. Geochronol.* 1, 74–85.
- Mouginot, J., Rignot, E., Scheuchl, B., 2014. Sustained increase in ice discharge from the Amundsen Sea Embayment, West Antarctica, from 1973 to 2013. *Geophys. Res. Lett.* 41, 1576–1584.
- Nishiizumi, K., 2004. Preparation of ^{26}Al AMS standards. *Nucl. Instrum. Methods Phys. Res. B* 223–224, 388–392.
- Nishiizumi, K., Imamura, M., Caffee, M.W., Southon, J.R., Finkel, R.C., McAninch, J., 2007. Absolute calibration of ^{10}Be AMS standards. *Nucl. Instrum. Methods Phys. Res. B* 258, 403–413.
- O Cofaigh, C., Evans, D.J.A., Smith, I.R., 2010. Large-scale reorganization and sedimentation of terrestrial ice streams during late Wisconsinan Laurentide Ice Sheet deglaciation. *Geol. Soc. Am. Bull.* 122, 743–756.
- Pankhurst, R.J., Weaver, S.D., Bradshaw, J.D., Storey, B.C., Ireland, T.R., 1998. Geochronology and geochemistry of pre-Jurassic superterraces in Marie Byrd Land, Antarctica. *J. Geophys. Res.* 103, 2529–2547.
- Peltier, W.R., Fairbanks, R.G., 2006. Global glacial ice volume and Last Glacial Maximum duration from an extended Barbados sea level record. *Quat. Sci. Rev.* 25, 3322–3337.
- Pollard, D., DeConto, R.M., 2009. Modelling West Antarctic ice sheet growth and collapse through the past five million years. *Nature* 458, 329–333.
- Pollard, D., Chang, W., Haran, M., Applegate, P., DeConto, R., 2016. Large-ensemble modelling of last deglacial retreat of the West Antarctic Ice Sheet: comparison of simple and advanced statistical techniques. *Geosci. Model. Dev.* 9, 1697–1723.
- Pritchard, H.D., Arthern, R.J., Vaughan, D.G., Edwards, L.A., 2009. Extensive dynamic thinning on the margins of the Greenland and Antarctic ice sheets. *Nature* 461, 971–975.
- Putnam, A.E., Denton, G.H., Schaefer, J.M., Barrell, D.J.A., Andersen, B.G., Finkel, R.C., Schwartz, R., Doughty, A.M., Kaplan, M.R., Schlüchter, C., 2010. *In situ* cosmogenic ^{10}Be production-rate calibration from the Southern Alps, New Zealand. *Quat. Geochronol.* 5, 392–409.
- RAISED Consortium, 2014. A community-based geological reconstruction of Antarctic Ice Sheet deglaciation since the Last Glacial Maximum. *Quat. Sci. Rev.* 100, 1–9.
- Rignot, E., Mouginot, J., Scheuchl, B., 2011a. Ice flow of the Antarctic ice sheet. *Science* 333, 1427–1430.
- Rignot, E., Mouginot, J., Scheuchl, B., 2011b. MEaSUREs InSAR-based Antarctica Ice Velocity Map, Version 1. NASA National Snow and Ice Data Center Distributed Active Archive Center, Boulder, Colorado USA. <https://doi.org/10.5067/MEASURES/CRYOSPHERE/nsidc-0484.001> [23 August 2016].
- Rignot, E., Mouginot, J., Scheuchl, B., 2011c. Antarctic grounding line mapping from differential satellite radar interferometry. *Geophys. Res. Lett.* 38, L10504.
- Rignot, E., Mouginot, J., Morlighem, N., Seroussi, H., Scheuchl, B., 2014. Widespread, rapid grounding line retreat of Pine Island, Thwaites, Smith, and Kohler glaciers, West Antarctica, from 1992 to 2011. *Geophys. Res. Lett.* 41, 3502–3509. <https://doi.org/10.1002/2014GL060140>.
- Ritz, C., Edwards, T.L., Durand, G., Payne, A.J., Peyaud, V., Hindmarsh, R.C.A., 2015. Potential sea-level rise from Antarctic ice-sheet instability constrained by observations. *Nature* 528, 115–118.
- Schaefer, J.M., Denton, G.H., Kaplan, M., Putnam, A., Finkel, R.C., Barrell, D.J., Andersen, B.G., Schwartz, R., Mackintosh, R., Chinn, T., Schluchter, C., 2009. High-frequency Holocene glacier fluctuations in New Zealand differ from the northern signature. *Science* 324, 622–625.
- Shepherd, A., et al., 2012. A reconciled estimate of ice-sheet mass balance. *Science* 338, 1183–1189.
- Smith, J.A., Hillenbrand, C.-D., Kuhn, G., Larter, R.D., Graham, A.G.C., Ehrmann, W.,

- Moreton, S.G., Forwick, M., 2011. Deglacial history of the West Antarctic Ice Sheet in the western Amundsen Sea Embayment. *Quat. Sci. Rev.* 30, 488–505.
- Smith, J.A., Hillenbrand, C.-D., Kuhn, G., Klages, J.P., Graham, A.G.C., Larter, R.D., Ehrmann, W., Moreton, S.G., Wiers, S., Frederichs, T., 2014. New constraints on the timing of West Antarctic Ice Sheet retreat in the eastern Amundsen Sea since the Last Glacial Maximum. *Glob. Planet. Change* 112, 224–237.
- Spector, P., Stone, J., Cowdery, S.G., Hall, B., Conway, H., Bromley, G., 2017. Rapid early-Holocene deglaciation in the Ross Sea, Antarctica. *Geophys. Res. Lett.* 44, 7817–7825.
- Stone, J.O., 2000. Air pressure and cosmogenic isotope productions. *J. Geophys. Res.* 105 (B10), 23753–23759.
- Stone, J.O., Balco, G., Sugden, D., Caffee, M., Sass III, L., Cowdery, S., Siddoway, C., 2003. Holocene deglaciation of Marie Byrd land, West Antarctica. *Science* 299, 99–102.
- WAIS Divide Project Members, 2013. Onset of deglacial warming in West Antarctica driven by local orbital forcing. *Nature* 500, 440–444.
- WAIS Divide Project Members, 2015. Precise interglacial phasing of abrupt climate change during the last ice age. *Nature* 520, 661–665.
- White, D., Fülöp, R.-H., Bishop, P., Mackintosh, A., Cook, G., 2011. Can *in-situ* cosmogenic ^{14}C be used to assess the influence of clast recycling on exposure dating of ice retreat in Antarctica? *Quat. Geochronol.* 6, 289–294.
- Whitehouse, P.L., Bentley, M.J., LeBrocq, A.M., 2012. A deglacial model for Antarctica: geological constraints and glaciological modelling as a basis for a new model of Antarctic glacial isostatic adjustment. *Quat. Sci. Rev.* 32, 1–24.